First Measurement of Λ_c Baryon Production in Au + Au Collisions at $\sqrt{s_{NN}} = 200$ GeV

J. Adam,[6] L. Adamczyk,[2] J. R. Adams,[39] J. K. Adkins,[30] G. Agakishiev,[28] M. M. Aggarwal,[40] Z. Ahammed,[59] I. Alekseev,[3,35] D. M. Anderson,[53] A. Aparin,[28] E. C. Aschenauer,[6] M. U. Ashraf,[11] F. G. Atetalla,[29] A. Attri,[40] G. S. Averichev,[28] V. Bairathi,[22] K. Barish,[10] A. Behera,[51] R. Bellwied,[20] A. Bhasin,[27] J. Bielcik,[14] J. Bielcikova,[38] L. C. Bland,[6] I. G. Bordyuzhin,[3] J. D. Brandenburg,[48,6] A. V. Brandin,[35] J. Butterworth,[44] H. Caines,[62] M. Calderón de la Barca Sánchez,[8] D. Cebra,[8] I. Chakaberia,[29,6] P. Chaloupka,[14] B. K. Chan,[9] F-H. Chang,[37] Z. Chang,[6] N. Chankova-Bunzarova,[28] A. Chatterjee,[11] D. Chen,[10] J. H. Chen,[18] X. Chen,[47] Z. Chen,[48] J. Cheng,[55] M. Cherney,[13] M. Chevalier,[10] S. Choudhury,[18] W. Christie,[6] H. J. Crawford,[7] M. Csanád,[16] M. Daugherity,[1] T. G. Dedovich,[28] I. M. Deppner,[19] A. A. Derevschikov,[42] L. Didenko,[6] X. Dong,[31] J. L. Drachenberg,[1] J. C. Dunlop,[6] T. Edmonds,[43] N. Elsey,[61] J. Engelage,[7] G. Eppley,[44] R. Esha,[51] S. Esumi,[56] O. Evdokimov,[12] J. Ewigleben,[32] O. Eyser,[6] R. Fatemi,[30] S. Fazio,[6] P. Federic,[38] J. Fedorisin,[28] C. J. Feng,[37] Y. Feng,[43] P. Filip,[28] E. Finch,[50] Y. Fisyak,[6] A. Francisco,[62] L. Fulek,[2] C. A. Gagliardi,[53] T. Galatyuk,[15] F. Geurts,[44] A. Gibson,[58] K. Gopal,[23] D. Grosnick,[58] W. Guryn,[6] A. I. Hamad,[29] A. Hamed,[5] J. W. Harris,[62] W. He,[18] X. He,[26] S. Heppelmann,[8] S. Heppelmann,[41] N. Herrmann,[19] E. Hoffman,[20] L. Holub,[14] Y. Hong,[31] S. Horvat,[62] Y. Hu,[18] H. Z. Huang,[9] S. L. Huang,[51] T. Huang,[37] X. Huang,[55] T. J. Humanic,[39] P. Huo,[51] G. Igo,[9] D. Isenhower,[1] W. W. Jacobs,[25] C. Jena,[23] A. Jentsch,[6] Y. JI,[47] J. Jia,[6,51] K. Jiang,[47] S. Jowzaee,[61] X. Ju,[47] E. G. Judd,[7] S. Kabana,[29] M. L. Kabir,[10] S. Kagamaster,[32] D. Kalinkin,[25] K. Kang,[55] D. Kapukchyan,[10] K. Kauder,[6] H. W. Ke,[6] D. Keane,[29] A. Kechechyan,[28] M. Kelsey,[31] Y. V. Khyzhniak,[35] D. P. Kikoła,[60] C. Kim,[10] B. Kimelman,[8] D. Kincses,[16] T. A. Kinghorn,[8] I. Kisel,[17] A. Kiselev,[6] A. Kisiel,[60] M. Kocan,[14] L. Kochenda,[35] L. K. Kosarzewski,[14] L. Kramarik,[14] P. Kravtsov,[35] K. Krueger,[4] N. Kulathunga Mudiyanselage,[20] L. Kumar,[40] R. Kunnawalkam Elayavalli,[61] J. H. Kwasizur,[25] R. Lacey,[51] S. Lan,[11] J. M. Landgraf,[6] J. Lauret,[6] A. Lebedev,[6] R. Lednicky,[28] J. H. Lee,[6] Y. H. Leung,[31] C. Li,[47] W. Li,[49] W. Li,[44] X. Li,[47] Y. Li,[55] Y. Liang,[29] R. Licenik,[38] T. Lin,[53] Y. Lin,[11] M. A. Lisa,[39] F. Liu,[11] H. Liu,[25] P. Liu,[51] P. Liu,[49] T. Liu,[62] X. Liu,[39] Y. Liu,[53] Z. Liu,[47] T. Ljubicic,[6] W. J. Llope,[61] R. S. Longacre,[6] N. S. Lukow,[52] S. Luo,[12] X. Luo,[11] G. L. Ma,[49] L. Ma,[18] R. Ma,[6] Y. G. Ma,[49] N. Magdy,[12] R. Majka,[62] D. Mallick,[36] S. Margetis,[29] C. Markert,[54] H. S. Matis,[31] J. A. Mazer,[45] N. G. Minaev,[42] S. Mioduszewski,[53] B. Mohanty,[36] I. Mooney,[61] Z. Moravcova,[14] D. A. Morozov,[42] M. Nagy,[16] J. D. Nam,[52] Md. Nasim,[22] K. Nayak,[11] D. Neff,[9] J. M. Nelson,[7] D. B. Nemes,[62] M. Nie,[48] G. Nigmatkulov,[35] T. Niida,[56] L. V. Nogach,[42] T. Nonaka,[11] G. Odyniec,[31] A. Ogawa,[6] S. Oh,[62] V. A. Okorokov,[35] B. S. Page,[6] R. Pak,[6] A. Pandav,[36] Y. Panebratsev,[28] B. Pawlik,[2] D. Pawlowska,[60] H. Pei,[11] C. Perkins,[7] L. Pinsky,[20] R. L. Pintér,[16] J. Pluta,[60] J. Porter,[31] M. Posik,[52] N. K. Pruthi,[40] M. Przybycien,[2] J. Putschke,[61] H. Qiu,[26] A. Quintero,[52] S. K. Radhakrishnan,[29] S. Ramachandran,[30] R. L. Ray,[54] R. Reed,[32] H. G. Ritter,[31] J. B. Roberts,[44] O. V. Rogachevskiy,[28] J. L. Romero,[8] L. Ruan,[6] J. Rusnak,[38] N. R. Sahoo,[48] H. Sako,[56] S. Salur,[45] J. Sandweiss,[62] S. Sato,[56] W. B. Schmidke,[6] N. Schmitz,[33] B. R. Schweid,[51] F. Seck,[15] J. Seger,[13] M. Sergeeva,[9] R. Seto,[10] P. Seyboth,[33] N. Shah,[24] E. Shahaliev,[28] P. V. Shanmuganathan,[6] M. Shao,[47] F. Shen,[48] W. Q. Shen,[49] S. S. Shi,[11] Q. Y. Shou,[49] E. P. Sichtermann,[31] R. Sikora,[2] M. Simko,[38] J. Singh,[40] S. Singha,[26] N. Smirnov,[62] W. Solyst,[25] P. Sorensen,[6] H. M. Spinka,[4] B. Srivastava,[43] T. D. S. Stanislaus,[58] M. Stefaniak,[60] D. J. Stewart,[62] M. Strikhanov,[35] B. Stringfellow,[43] A. A. P. Suaide,[46] M. Sumbera,[38] B. Summa,[41] X. M. Sun,[11] Y. Sun,[47] Y. Sun,[21] B. Surrow,[52] D. N. Svirida,[3] P. Szymanski,[60] A. H. Tang,[6] Z. Tang,[47] A. Taranenko,[35] T. Tarnowsky,[34] J. H. Thomas,[31] A. R. Timmins,[20] D. Tlusty,[13] M. Tokarev,[28] C. A. Tomkiel,[32] S. Trentalange,[9] R. E. Tribble,[53] P. Tribedy,[6] S. K. Tripathy,[16] O. D. Tsai,[9] Z. Tu,[6] T. Ullrich,[6] D. G. Underwood,[4] I. Upsal,[48,6] G. Van Buren,[6] J. Vanek,[38] A. N. Vasiliev,[42] I. Vassiliev,[17] F. Videbæk,[6] S. Vokal,[28] S. A. Voloshin,[61] F. Wang,[43] G. Wang,[9] J. S. Wang,[21] P. Wang,[47] Y. Wang,[11] Y. Wang,[55] Z. Wang,[48] J. C. Webb,[6] P. C. Weidenkaff,[19] L. Wen,[9] G. D. Westfall,[34] H. Wieman,[31] S. W. Wissink,[25] R. Witt,[57] Y. Wu,[10] Z. G. Xiao,[55] G. Xie,[31] W. Xie,[43] H. Xu,[21] N. Xu,[31] Q. H. Xu,[48] Y. F. Xu,[49] Y. Xu,[48] Z. Xu,[6] Z. Xu,[9] C. Yang,[48] Q. Yang,[48] S. Yang,[6] Y. Yang,[37] Z. Yang,[11] Z. Ye,[44] Z. Ye,[12] L. Yi,[48] K. Yip,[6] H. Zbroszczyk,[60] W. Zha,[47] D. Zhang,[11] S. Zhang,[47] S. Zhang,[49] X. P. Zhang,[55] Y. Zhang,[47] Z. J. Zhang,[37] Z. Zhang,[6] J. Zhao,[43] C. Zhong,[49] C. Zhou,[49] X. Zhu,[55] Z. Zhu,[48] M. Zurek,[31] and M. Zyzak[17]

(STAR Collaboration)

[1]*Abilene Christian University, Abilene, Texas 79699*
[2]*AGH University of Science and Technology, FPACS, Cracow 30-059, Poland*
[3]*Alikhanov Institute for Theoretical and Experimental Physics NRC "Kurchatov Institute," Moscow 117218, Russia*

[4]Argonne National Laboratory, Argonne, Illinois 60439
[5]American University of Cairo, New Cairo 11835, Egypt
[6]Brookhaven National Laboratory, Upton, New York 11973
[7]University of California, Berkeley, California 94720
[8]University of California, Davis, California 95616
[9]University of California, Los Angeles, California 90095
[10]University of California, Riverside, California 92521
[11]Central China Normal University, Wuhan, Hubei 430079
[12]University of Illinois at Chicago, Chicago, Illinois 60607
[13]Creighton University, Omaha, Nebraska 68178
[14]Czech Technical University in Prague, FNSPE, Prague 115 19, Czech Republic
[15]Technische Universität Darmstadt, Darmstadt 64289, Germany
[16]ELTE Eötvös Loránd University, Budapest, Hungary H-1117
[17]Frankfurt Institute for Advanced Studies FIAS, Frankfurt 60438, Germany
[18]Fudan University, Shanghai, 200433
[19]University of Heidelberg, Heidelberg 69120, Germany
[20]University of Houston, Houston, Texas 77204
[21]Huzhou University, Huzhou, Zhejiang 313000
[22]Indian Institute of Science Education and Research (IISER), Berhampur 760010, India
[23]Indian Institute of Science Education and Research (IISER) Tirupati, Tirupati 517507, India
[24]Indian Institute Technology, Patna, Bihar 801106, India
[25]Indiana University, Bloomington, Indiana 47408
[26]Institute of Modern Physics, Chinese Academy of Sciences, Lanzhou, Gansu 730000
[27]University of Jammu, Jammu 180001, India
[28]Joint Institute for Nuclear Research, Dubna 141 980, Russia
[29]Kent State University, Kent, Ohio 44242
[30]University of Kentucky, Lexington, Kentucky 40506-0055
[31]Lawrence Berkeley National Laboratory, Berkeley, California 94720
[32]Lehigh University, Bethlehem, Pennsylvania 18015
[33]Max-Planck-Institut für Physik, Munich 80805, Germany
[34]Michigan State University, East Lansing, Michigan 48824
[35]National Research Nuclear University MEPhI, Moscow 115409, Russia
[36]National Institute of Science Education and Research, HBNI, Jatni 752050, India
[37]National Cheng Kung University, Tainan 70101
[38]Nuclear Physics Institute of the CAS, Rez 250 68, Czech Republic
[39]Ohio State University, Columbus, Ohio 43210
[40]Panjab University, Chandigarh 160014, India
[41]Pennsylvania State University, University Park, Pennsylvania 16802
[42]NRC "Kurchatov Institute," Institute of High Energy Physics, Protvino 142281, Russia
[43]Purdue University, West Lafayette, Indiana 47907
[44]Rice University, Houston, Texas 77251
[45]Rutgers University, Piscataway, New Jersey 08854
[46]Universidade de São Paulo, São Paulo, Brazil 05314-970
[47]University of Science and Technology of China, Hefei, Anhui 230026
[48]Shandong University, Qingdao, Shandong 266237
[49]Shanghai Institute of Applied Physics, Chinese Academy of Sciences, Shanghai 201800
[50]Southern Connecticut State University, New Haven, Connecticut 06515
[51]State University of New York, Stony Brook, New York 11794
[52]Temple University, Philadelphia, Pennsylvania 19122
[53]Texas A&M University, College Station, Texas 77843
[54]University of Texas, Austin, Texas 78712
[55]Tsinghua University, Beijing 100084
[56]University of Tsukuba, Tsukuba, Ibaraki 305-8571, Japan
[57]United States Naval Academy, Annapolis, Maryland 21402
[58]Valparaiso University, Valparaiso, Indiana 46383
[59]Variable Energy Cyclotron Centre, Kolkata 700064, India

[60]Warsaw University of Technology, Warsaw 00-661, Poland
[61]Wayne State University, Detroit, Michigan 48201
[62]Yale University, New Haven, Connecticut 06520

(Received 1 November 2019; revised manuscript received 24 February 2020; accepted 27 March 2020; published 1 May 2020)

We report on the first measurement of the charmed baryon $\Lambda_c^\pm$ production at midrapidity ($|y| < 1$) in Au + Au collisions at $\sqrt{s_{\rm NN}} = 200$ GeV collected by the STAR experiment at the Relativistic Heavy Ion Collider. The Λ_c/D^0 [denoting $(\Lambda_c^+ + \Lambda_c^-)/(D^0 + \bar{D}^0)$] yield ratio is measured to be 1.08 ± 0.16 (stat) $\pm$ 0.26 (sys) in the 0%–20% most central Au + Au collisions for the transverse momentum (p_T) range $3 < p_T < 6$ GeV/c. This is significantly larger than the PYTHIA model calculations for $p + p$ collisions. The measured Λ_c/D^0 ratio, as a function of p_T and collision centrality, is comparable to the baryon-to-meson ratios for light and strange hadrons in Au + Au collisions. Model calculations including coalescence hadronization for charmed baryon and meson formation reproduce the features of our measured Λ_c/D^0 ratio.

DOI: 10.1103/PhysRevLett.124.172301

Heavy-ion collisions offer a unique opportunity to study quantum chromodynamics (QCD), the theory describing strong interactions between quarks and gluons through color charges. Data collected from the Relativistic Heavy Ion Collider (RHIC) and the Large Hadron Collider (LHC) demonstrate that novel QCD matter, quark-gluon plasma (QGP), in which quarks and gluons are deconfined, is created in high-energy nucleus-nucleus collisions [1,2]. QCD hadronization is a nonperturbative process and remains a challenging process to model. Fragmentation fractions measured in high-energy ee, ep, and pp collisions have been used to successfully describe hadron production at high transverse momentum (p_T) and are deployed in Monte Carlo event generators like PYTHIA [3] using a string fragmentation hadronization scheme. Recently, different schemes, such as color reconnection (CR) in PYTHIA, where strings from different multiparton interactions are allowed to recombine, have been developed to reproduce the low-p_T hadron data, including an enhanced production of baryons, in pp collisions [4]. In central heavy-ion collisions, baryon-to-meson ratios for light and strange hadrons in $2 < p_T < 6$ GeV/c show an enhancement compared to pp collisions [5–7]. A coalescence hadronization mechanism, in which hadrons can be formed via recombination of close-by partons in phase space in the deconfined QGP, has been utilized to describe the enhancement in heavy-ion collisions [8,9]. Alternatively to these microscopic schemes, a statistical hadronization scheme, which determines hadron yields statistically by their quantum numbers and thermal properties of the system, is used to fit successfully various light and strange hadron integrated yields in ee, pp, and heavy-ion collisions [10].

Because of their large masses, heavy quarks (c and b) are predominately created from initial hard scatterings in heavy-ion collisions. The relative yields of heavy-flavor hadrons can serve as a tag to study their hadronization process. The c quark fragmentation fraction ratio $(c \to \Lambda_c^+)/(c \to D^0)$ was measured to be around 0.10–0.15 in ee and ep collisions [11–13]. Recently, ALICE and LHCb measured [14,15] the Λ_c/D^0 ratio in $p + p$ and $p +$ Pb collisions at the LHC to be 0.4–0.5 at $2 < p_T < 8$ GeV/c, larger than the PYTHIA model calculation based on string fragmentation. The PYTHIA model with color reconnection yields a larger Λ_c/D^0 ratio that is close to the data [14].

In heavy-ion collisions, models including coalescence hadronization of charm quarks predict a large Λ_c/D^0 ratio of $\sim$1, in the low to intermediate p_T regions ($< \sim$8 GeV/c) [16–18]. The ALICE Collaboration reported the Λ_c/D^0 ratio to be $\sim$1 at $6 < p_T < 12$ GeV/c in Pb + Pb collisions at $\sqrt{s_{\rm NN}} = 5.02$ TeV, consistent with a contribution of coalescence hadronization for charm quarks [19]. Measurement of $\Lambda_c^\pm$ production in heavy-ion collisions over a broad momentum region, particularly at lower p_T, will offer significant insights into the hadronization mechanism of charm quarks in the presence of a QGP. Furthermore, understanding the hadronization mechanism of charm quarks in heavy-ion collisions is crucial to the study of charm-quark energy loss in the QGP using the measurements of nuclear modification factors ($R_{\rm AA}$) of D mesons [20–22] in heavy-ion collisions. Since the charm quarks are dominantly produced through initial hard scatterings, a large baryon-to-meson ratio directly impacts the charm meson $R_{\rm AA}$.

In this Letter, we report on the first measurement of $\Lambda_c^\pm$ production in Au + Au collisions at $\sqrt{s_{\rm NN}} = 200$ GeV. The analysis is carried out at midrapidity ($|y| < 1$) and utilized a total of 2.3 billion minimum bias (MB) triggered events collected by the STAR experiment during 2014 and 2016 runs at RHIC. The heavy flavor tracker (HFT) [23], a four-layer high-resolution silicon detector, was used for excellent vertex resolution that improves significantly the signal-to-background ratio for charmed hadron reconstruction. The MB events are selected by requiring a coincidence between the east and west vertex position detectors [24]. The events are required to have the reconstructed primary vertex (PV) position along the beam direction within 6 cm from the detector center, to ensure

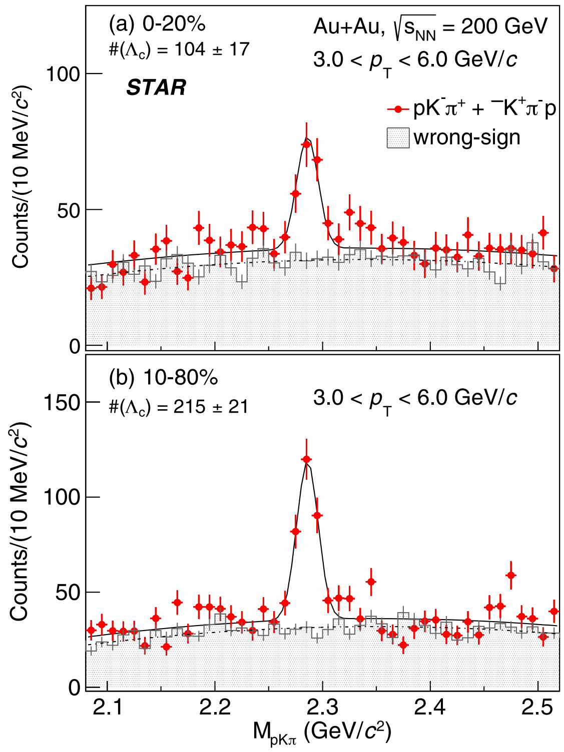

FIG. 1. The $pK\pi$ invariant mass distributions for right-sign (solid red points) and wrong-sign (shaded histograms) combinations in Au + Au collisions at $\sqrt{s_{\mathrm{NN}}} = 200$ GeV for 0%–20% (top) and 10%–80% (bottom) centrality classes. The wrong-sign distributions are scaled by $1/3$, the ratio of the number of right-sign to wrong-sign combinations for the $pK\pi$ triplet. The error bars shown are statistical uncertainties. The solid line depicts a fit with a Gaussian function, for a $\Lambda_c^{\pm}$ signal, and a second-order polynomial function, the shape of which is fixed by fit to the wrong-sign distribution (dashed line), for the background.

good HFT acceptance. The collision centrality, a measure of the geometric overlap between the two colliding nuclei, is defined using the measured charged track multiplicity at midrapidity, as compared to a Monte Carlo Glauber simulation [25].

The $\Lambda_c^{\pm}$ baryons are reconstructed via the hadronic decay channel $\Lambda_c^{+} \to K^{-}\pi^{+}p$ and its charge conjugate. Charged particle tracks are reconstructed from hits in the STAR time projection chamber (TPC) [26] and HFT detectors, in a 0.5 T magnetic field. Tracks are required to have a minimum of 20 TPC hits (out of a maximum of 45) and at least three hits in the HFT subdetectors. The tracks are also required to be within pseudorapidity $|\eta| < 1$ with $p_T > 0.5$ GeV$/c$. Particle identification (PID) is achieved by a combination of the ionization energy loss dE/dx, measured by the TPC, and the timing, measured by the time of flight detector [27].

The $\Lambda_c^{\pm}$ decay vertex is reconstructed as the midpoint of the distance of closest approach (DCA) between the three daughter tracks. To improve separation of the signal from combinatorial background of tracks originating from the primary vertex, we utilized a supervised machine learning algorithm, the boosted decision trees (BDTs), implemented in the TMVA package [28]. The BDTs are trained with a signal sample of $\Lambda_c^{\pm} \to K\pi p$ decays simulated using the EvtGen generator [29] with detector effects taken into account and a background sample of wrong-sign $K\pi p$ combinations from data. The variables characterizing the decay topology, viz. the decay length, DCA of daughter tracks to the PV, and the DCA of the reconstructed Λ_c candidate to the PV are used as input variables in the training. The cut on BDT response is optimized for maximum $\Lambda_c^{\pm}$ signal significance using the estimated number of signal and background $\Lambda_c^{\pm}$ candidates in the data. Figure 1 shows examples of invariant mass distributions with the BDT selection, of $K\pi p$ triplets with the right and wrong sign (scaled by $1/3$) combinations. The distributions in the 0%–20% most central collisions (top) and the 10%–80% central collisions (bottom), the centrality range used for p_T-dependent measurement, are shown. The right-sign distributions are fit to a Gaussian for the signal plus a second-order polynomial for the background, with the shape of the polynomial function fixed from fitting to the wrong-sign distribution. The raw signal yields are obtained as the counts of the right-sign triplets within a mass window of three standard deviations of the Gaussian fit with background counts, evaluated using the polynomial component of the fit in the same mass window, subtracted.

The $\Lambda_c^{\pm}$ reconstruction efficiency is evaluated using a hybrid method, similarly to the D^0 spectra measurement with the STAR HFT [20]. The TPC tracking efficiency is obtained using the standard embedding technique used in many other STAR analyses [30]. The PID efficiencies are evaluated using pure π, K, and p samples from the data. The HFT tracking and the BDT selection efficiency are calculated using a data-driven simulation framework with the input distributions taken from the real data. The input distributions include the TPC-to-HFT matching efficiency (the fraction of good TPC tracks matched to hits in HFT) and the DCA distributions of tracks with respect to the reconstructed collision vertex. Protons reconstructed in the real data have a sizable secondary contribution from other hyperon decays, which impacts the TPC-to-HFT matching ratio and DCA distributions. A correction factor to the efficiency calculated using the data-driven simulation is evaluated using Au + Au events from HIJING [31] propagated through the STAR GEANT detector geometry [32] and digital signals embedded into those from zero-bias data (denoted HIJING + ZB). Zero-bias data consist of events taken with no collision requirement and capture the background conditions in the detectors during the run. The p_T distributions of protons and hyperons from HIJING are reweighted to match the data [5,30]. The events are then reconstructed with the same algorithm as the real data. The correction is calculated as a ratio of the efficiency from the data-driven simulation, using the input distributions for

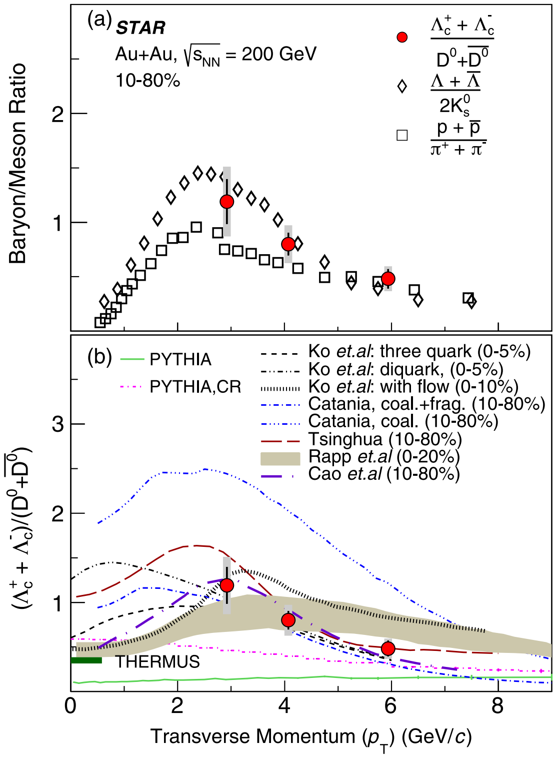

FIG. 2. The measured Λ_c/D^0 ratio at midrapidity ($|y| < 1$) as a function of p_T for Au + Au collisions at $\sqrt{s_{NN}} = 200$ GeV in 10%–80% centrality, compared to the baryon-to-meson ratios for light and strange hadrons (top) and various model calculations (bottom). The vertical lines and shaded boxes on the Λ_c/D^0 data points indicate statistical and systematic uncertainties, respectively. The p_T integrated Λ_c/D^0 ratio from the THERMUS [10] model calculation with a freeze-out temperature of $T_{ch} = 160$ MeV is shown as a horizontal bar on the left axis of the plot.

inclusive tracks from the reconstructed HIJING + ZB data, to the one using inputs from primary tracks from the same data. The correction factor is found to be about 30% with very weak p_T and centrality dependences. The impact of the finite primary vertex resolution on the reconstruction efficiency obtained by this method is also evaluated using the HIJING + ZB events with procedures similar to those described in Ref. [20]. It is found to be within 10% for the 50%–80% centrality class and negligible for more central events. The yields are finally corrected for the $\Lambda_c^\pm \to K\pi p$ branching ratio (BR) of $6.28 \pm 0.32\%$ [33].

The systematic uncertainties to the measurement include the uncertainties in raw yield extraction and various efficiency correction factors. The former is evaluated by varying the background estimation method (varying the fit range and choice of background function and leaving the background shape unconstrained) and is between 6% and 14% in the measured p_T region. The contribution to the yield under the mass peak from incorrectly assigned PID for daughter tracks is less than 1%. The TPC efficiency uncertainty is evaluated to be ~15%, and PID efficiency uncertainties to be ~6%, for three daughter tracks combined. The uncertainty in the HFT tracking and topological cut efficiency is estimated by changing the BDT response cuts so that the reconstruction efficiency varies by 50% above and below relative to the nominal one. The resulting nonstatistical variations to final results are included in the systematic uncertainties and range from 10% to 15%. For the correction factor due to secondary protons, the uncertainties from the measured proton and Λ spectra [5,30], as well as those on other hadrons that decay to protons, are propagated. This uncertainty is estimated to be about 4%. We also include a 10% uncertainty from a closure test for the data-driven simulation method, evaluated by comparing the efficiencies calculated using a data-driven simulation with input distributions from reconstructed HIJING + ZB events, to the efficiencies evaluated directly from the reconstructed HIJING + ZB events. The feed-down contribution from bottom hadrons to the measurements is found to be small and less than 4% in the measured p_T range. Finally, the uncertainty in the decay BR from the latest PDG [33] value is added as a global normalization uncertainty in the $\Lambda_c^\pm$ yield.

The $\Lambda_c^\pm$ invariant yields in the 10%–80% centrality class for the different p_T bins are shown in Table I, along with the statistical and systematic uncertainties. The 10%–80% centrality class is chosen for p_T-dependent measurement, as it had the best Λ_c signal significance in the measured regions. The ratio of the invariant yield of $\Lambda_c^\pm$ to that of D^0 is shown as a function of p_T in Fig. 2 for the 10%–80% centrality class. The correlated systematic uncertainties from efficiency correction that go into both $\Lambda_c^\pm$ and D^0 measurements cancel. Figure 2(a) compares the Λ_c/D^0 ratio to the baryon-to-meson ratios from light and strange-flavor hadrons [5,30]. The Λ_c/D^0 ratio is comparable in magnitude to the Λ/K_s^0 and p/π ratios and shows a similar p_T dependence in the measured region.

The measured values are compared to different model calculations in Fig. 2(b). The values show a significant enhancement compared to the calculations from the latest PYTHIA 8.24 release (Monash tune [34]) without CR [4]. The implementation with CR (mode2 in Ref. [4]) enhances the baryon production with respect to mesons and gives a Λ_c/D^0 yield ratio consistent with those measured in $p + p$ and p + Pb collisions at the LHC [14,15]. However, both calculations fail to fully describe the Au + Au data and their p_T dependence. The mode without CR is ruled out at a p value of 1×10^{-4} (χ^2/NDF = 20.7/3), while the CR mode gives a p value of 0.04 (χ^2/NDF = 8.2/3) using a reduced χ^2 test.

Figure 2(b) shows the comparison to calculations from various models that include coalescence hadronization of charm quarks (labeled Ko *et al.* with three quarks and diquarks [16], Ko *et al.* with flow [35], Catania [36], Tsinghua [37], Rapp *et al.* [38], and Cao *et al.* [39]). The models differ among themselves in the choice of hadron

TABLE I. The $\Lambda_c^{\pm}$ invariant yields measured in the 10%–80% centrality class for the different p_T bins, in Au + Au collisions at $\sqrt{s_{NN}} = 200$ GeV.

p_T (GeV/c)	$1/(2\pi p_T N_{evt}) d^2N/dp_T dy$ (GeV/c)$^{-2}$
2.5–3.5	$8.2\times10^{-4} \pm 1.4\times10^{-4}$ (stat) $\pm 2.4\times10^{-4}$ (sys)
3.5–5.0	$6.0\times10^{-5} \pm 7.7\times10^{-6}$ (stat) $\pm 1.5\times10^{-5}$ (sys)
5.0–8.0	$2.1\times10^{-6} \pm 3.8\times10^{-7}$ (stat) $\pm 5.5\times10^{-7}$ (sys)

wave functions, light- and charm-quark spectra in the QGP, and also treatment of space-time correlations during coalescence and excited states that decay into Λ_c and D^0 that are considered. Most of the models are able to give enhanced Λ_c/D^0 yield ratios and describe the measured p_T dependence of the ratio. A reduced χ^2 test is carried out, taking into account the finite p_T bin width in the measurement. The Catania model calculations of the Λ_c/D^0 ratio from hadrons formed only through coalescence hadronization overpredict the measurement at all p_T (reduced $\chi^2 = 26.1$). The calculations from Ko *et al.* with flow give a reduced χ^2 value of 4.8, mainly from the overprediction of the ratio in the highest two p_T bins. The other coalescence model calculations are consistent with the data within uncertainties over the measured p_T range. It should be noted that the calculations from Rapp *et al.* and Ko *et al.* have different centrality ranges than in the measurement, which may impact the χ^2 values quoted. In the models discussed above, charm-quark radial flow is implicitly included mainly through the charm-quark diffusion in the medium. However, it was found that a purely radial flow effect without coalescence hadronization, evaluated using a blast-wave model with freeze-out parameters from D^0 measurement [20], causes the Λ_c/D^0 ratio to rise strongly with increasing p_T in the measured p_T region. This is similar to the behavior observed for light hadrons [6] and opposite to the trend measured in the data. The comparisons favor coalescence hadronization as having an important role in charm-quark hadronization in the presence of QGP. The data offer constraints to the model parameters and to the coalescence probabilities of charm quarks in the medium.

The p_T-integrated Λ_c/D^0 ratio is calculated to be 0.80 ± 0.12 (stat) ± 0.22 (sys, data) ± 0.41 (sys, model). The coalescence model curves shown in Fig. 2(b) were used to extrapolate to $p_T = 0$ GeV/c, with the mean of the extrapolated values from different models taken as the central value and the maximum difference between them included in the systematic uncertainty. The ratio is consistent, including extrapolation uncertainties, with the value (0.35) from the thermal model calculation using THERMUS [10] with a freeze-out temperature $T_{ch} = 160$ MeV. This suggests $\Lambda_c^{\pm}$ contribute sizably to the total charm yield in heavy-ion collisions.

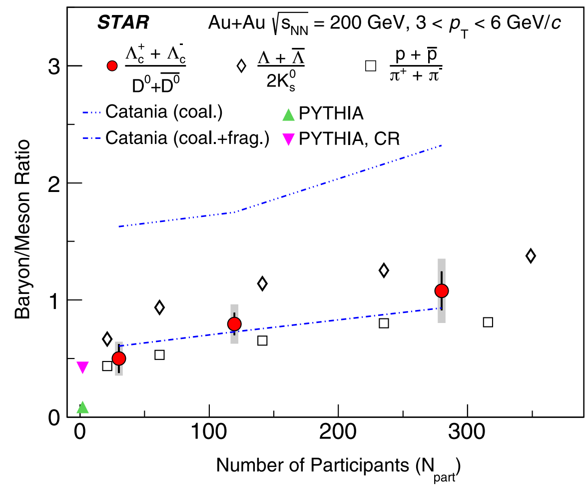

FIG. 3. The measured Λ_c/D^0 yield ratio in $3 < p_T < 6$ GeV/c (solid circles) as a function of collision centrality (expressed in N_{part}) for Au + Au collisions at $\sqrt{s_{NN}} = 200$ GeV. The open diamonds and squares show the baryon-to-meson ratio measured for strange and light-flavor hadrons, respectively. The vertical lines and the shaded boxes on the Λ_c/D^0 data points indicate statistical and systematic uncertainties, respectively. The dashed curves indicate the Λ_c/D^0 ratio calculated from a model with charm-quark coalescence, and the up and down triangles indicate the ratios from the PYTHIA model for $p + p$ collisions without and with CR respectively, for the same p_T region.

The centrality dependence of the Λ_c/D^0 ratio, plotted as a function of the number of participant nucleons N_{part}, for $3 < p_T < 6$ GeV/c is shown in Fig. 3. The measurements correspond to the centrality ranges 50%–80%, 20%–50%, and 0%–20%. The Λ_c/D^0 ratio shows an increase toward more central collisions. The increasing trend is qualitatively similar to that seen for the baryon-to-meson ratio for light and strange-flavor hadrons and to that predicted by coalescence model calculations. The measured Λ_c/D^0 ratio in 0%–20% central collisions of 1.08 ± 0.16 (stat) $\pm$ 0.26 (sys) is larger than the values from PYTHIA 8.2 without CR (at 3.1σ significance) and with CR (at 2.1σ significance).

In summary, STAR reports on the first measurement of $\Lambda_c^{\pm}$ baryon production in Au + Au collisions at $\sqrt{s_{NN}} =$ 200 GeV utilizing its high-resolution silicon detector. The measured Λ_c/D^0 yield ratio at midrapidity ($|y| < 1$) is found to be comparable to the baryon-to-meson ratios for light and strange-flavor hadrons in the same kinematic regions. The large Λ_c/D^0 ratio also suggests that charmed baryons contribute significantly to the total charm cross section at midrapidity in heavy-ion collisions at RHIC. The Λ_c/D^0 ratio in Au + Au collisions is considerably larger than the PYTHIA expectation at the same energy. Several model calculations that include coalescence hadronization for charm hadron formation can reproduce the features of our data. Our data are expected to offer significant constraints toward the understanding of QCD hadronization in the finite temperature region and to the charm-quark transport and energy loss in the QGP.

We thank the RHIC Operations Group and RCF at BNL, the NERSC Center at LBNL, and the Open Science Grid consortium for providing resources and support. This work was supported in part by the Office of Nuclear Physics within the U.S. DOE Office of Science, the U.S. National Science Foundation, the Ministry of Education and Science of the Russian Federation, National Natural Science Foundation of China, Chinese Academy of Science, the Ministry of Science and Technology of China and the Chinese Ministry of Education, the National Research Foundation of Korea, Czech Science Foundation and Ministry of Education, Youth and Sports of the Czech Republic, Hungarian National Research, Development and Innovation Office, New National Excellency Programme of the Hungarian Ministry of Human Capacities, Department of Atomic Energy and Department of Science and Technology of the Government of India, the National Science Centre of Poland, the Ministry of Science, Education and Sports of the Republic of Croatia, RosAtom of Russia and German Bundesministerium fur Bildung, Wissenschaft, Forschung and Technologie (BMBF), and the Helmholtz Association.

[1] Y. Akiba *et al.*, arXiv:1502.02730.
[2] J. Adams *et al.* (STAR Collaboration), Nucl. Phys. **A757**, 102 (2005); K. Adcox *et al.* (PHENIX Collaboration), Nucl. Phys. **A757**, 184 (2005); B. B. Back *et al.*, Nucl. Phys. **A757**, 28 (2005); I. Arsene *et al.* (BRAHMS Collaboration), Nucl. Phys. **A757**, 1 (2005).
[3] T. Sjostrand, S. Mrenna, and P. Z. Skands, J. High Energy Phys. 05 (2006) 026.
[4] C. Bierlich and J. R. Christiansen, Phys. Rev. D **92**, 094010 (2015).
[5] B. I. Abelev *et al.* (STAR Collaboration), Phys. Rev. Lett. **97**, 152301 (2006).
[6] B. B. Abelev *et al.* (ALICE Collaboration), Phys. Rev. Lett. **111**, 222301 (2013).
[7] B. I. Abelev *et al.* (STAR Collaboration), Phys. Lett. B **655**, 104 (2007).
[8] Z. W. Lin and D. Molnar, Phys. Rev. C **68**, 044901 (2003).
[9] R. J. Fries, V. Greco, and P. Sorensen, Annu. Rev. Nucl. Part. Sci. **58**, 177 (2008).
[10] S. Wheaton, J. Cleymans, and M. Hauer, Comput. Phys. Commun. **180**, 84 (2009).
[11] R. Barate *et al.* (ALEPH Collaboration), Eur. Phys. J. C **16**, 597 (2000).
[12] H. Abramowicz *et al.* (ZEUS Collaboration), J. High Energy Phys. 09 (2013) 058.
[13] M. Lisovyi, A. Verbytskyi, and O. Zenaiev, EPJ Web Conf. **120**, 03002 (2016).
[14] S. Acharya *et al.* (ALICE Collaboration), J. High Energy Phys. 04 (2018) 108.
[15] R. Aaij *et al.* (LHCb Collaboration), J. High Energy Phys. 02 (2019) 102.
[16] Y. Oh, C. M. Ko, S. H. Lee, and S. Yasui, Phys. Rev. C **79**, 044905 (2009).
[17] V. Greco, C. M. Ko, and R. Rapp, Phys. Lett. B **595**, 202 (2004).
[18] S. H. Lee, K. Ohnishi, S. Yasui, I.-K. Yoo, and C.-M. Ko, Phys. Rev. Lett. **100**, 222301 (2008).
[19] S. Acharya *et al.* (ALICE Collaboration), Phys. Lett. B **793**, 212 (2019).
[20] J. Adam *et al.* (STAR Collaboration), Phys. Rev. C **99**, 034908 (2019).
[21] A. M. Sirunyan *et al.* (CMS Collaboration), Phys. Lett. B **782**, 474 (2018).
[22] J. Adam *et al.* (ALICE Collaboration), J. High Energy Phys. 03 (2016) 081.
[23] G. Contin *et al.*, Nucl. Instrum. Methods Phys. Res., Sect. A **907**, 60 (2018).
[24] W. J. Llope *et al.*, Nucl. Instrum. Methods Phys. Res., Sect. A **522**, 252 (2004).
[25] B. I. Abelev *et al.* (STAR Collaboration), Phys. Rev. C **79**, 034909 (2009).
[26] M. Anderson *et al.*, Nucl. Instrum. Methods Phys. Res., Sect. A **499**, 659 (2003).
[27] W. J. Llope (STAR Collaboration), Nucl. Instrum. Methods Phys. Res., Sect. A **661**, S110 (2012).
[28] A. Hoecker *et al.*, arXiv:physics/0703039.
[29] D. J. Lange, Nucl. Instrum. Methods Phys. Res., Sect. A **462**, 152 (2001).
[30] G. Agakishiev *et al.* (STAR Collaboration), Phys. Rev. Lett. **108**, 072301 (2012).
[31] M. Gyulassy and X.-N. Wang, Comput. Phys. Commun. **83**, 307 (1994).
[32] S. Agostinelli *et al.* (GEANT4 Collaboration), Nucl. Instrum. Methods Phys. Res., Sect. A **506**, 250 (2003).
[33] M. Tanabashi *et al.* (Particle Data Group), Phys. Rev. D **98**, 030001 (2018).
[34] P. Skands, S. Carrazza, and J. Rojo, Eur. Phys. J. C **74**, 3024 (2014).
[35] S. Cho, K.-J. Sun, C. M. Ko, S. H. Lee, and Y. Oh, Phys. Rev. C **101**, 024909 (2020).
[36] S. Plumari, V. Minissale, S. K. Das, G. Coci, and V. Greco, Eur. Phys. J. C **78**, 348 (2018).
[37] J. Zhao, S. Shi, N. Xu, and P. Zhuang, arXiv:1805.10858.
[38] M. He and R. Rapp, Phys. Rev. Lett. **124**, 042301 (2020).
[39] S. Cao, K.-J. Sun, S. Y. F. Liu, W.-J. Xing, G.-Y. Qin, and C.-M. Ko, arXiv:1911.00456.